Acta Crystallographica Section A
Foundations of Crystallography
ISSN 0108-7673

Received 19 February 2009
Accepted 26 April 2009

Investigations of the bond-selective response in a piezoelectric $Li_2SO_4{\cdot}H_2O$ crystal to an applied external electric field

O. Schmidt,[a]* S. Gorfman,[b] L. Bohatý,[c] E. Neumann,[d] B. Engelen[d] and U. Pietsch[a]

[a]Department of Physics, University of Siegen, Siegen, Germany, [b]Department of Physics, University of Warwick, Coventry, UK, [c]Institute of Crystallography, University of Cologne, Cologne, Germany, and [d]Department of Chemistry, University of Siegen, Siegen, Germany. Correspondence e-mail: oleg.schmidt@physik.uni-siegen.de

Piezoelectric lithium sulfate monohydrate, $Li_2SO_4{\cdot}H_2O$, was analyzed with respect to the relationship between the static structural properties of the crystal and its response to an external electric field. The static electron density was determined *via* standard low-temperature X-ray data collection at 90 (5) K using an Enraf–Nonius CAD-4 diffractometer, Mo $K\alpha$ radiation and multipole model refinement. Then a synchrotron-radiation experiment using the D3 beamline at HASYLAB was conducted in order to investigate the structural deformations in $Li_2SO_4{\cdot}H_2O$ caused by an applied external electric field. In particular, the shifts of Bragg-peak positions induced by the electric field were measured and the piezoelectric constants d_{211}, d_{222}, d_{233} and d_{213} of $Li_2SO_4{\cdot}H_2O$ were obtained from the shifts. With the same experimental setup the variations of more than 100 Bragg intensities were measured under an applied electric field. The data were used to refine the corresponding displacements of individual atoms within the unit cell. The distortions of the cation–anion bond lengths in the LiO_4, $LiO_3(H_2O)$ and SO_4 tetrahedra were evaluated and then analyzed in terms of the electron-density-related properties of the Li—O and S—O bonds. The two lithium structural units were found to be strongly deformed by the applied electric field, while the SO_4 tetrahedron changed less. This is in agreement with the low bond strength of the Li—O bonds.

1. Introduction

X-ray diffraction is the major experimental tool for the investigation of the microscopic structure of crystals. A highly redundant set of Bragg intensities can be collected almost automatically with high precision and can be used to obtain accurate atomic positions and atomic displacement parameters (ADPs) and the electron-density distribution. In general, these quantities describe the crystal at the static equilibrium, *i.e.* in the absence of any external influences. However, probing the microscopic response of a crystal to an external perturbation is still a challenge for modern X-ray structure analysis. The main aim of such experiments is to understand how specific features of the structural network are responsible for the physical properties of a crystal and how the crystal structural parameters can be tuned to control the property of interest.

The types of perturbations which are usually applied to a crystal in an X-ray diffraction experiment are high pressure, high or low temperatures, laser irradiation and external high voltage (Oganov *et al.*, 2006; Istomin *et al.*, 2007; Coppens & Novozhilova, 2002; Stahn *et al.*, 2001). The specific response of the crystal to such perturbations defines its intrinsic physical properties, *e.g.* the development of the macroscopic polarization under the influence of an applied electric field is known as dielectricity, whereas the formation of mechanical strains is referred to as the converse piezoelectric effect (Nye, 1957). Although many technical applications are essentially based on both of these phenomena, their microscopic nature is not yet well understood. Starting with the pioneering work by Fujimoto (1978) which was further continued by Paturle *et al.* (1991), Graafsma *et al.* (1993), van Reeuwijk *et al.* (2001), Stahn *et al.* (2001), Guillot *et al.* (2002), Davaasambuu *et al.* (2003), Guillot *et al.* (2004), Gorfman *et al.* (2006) and Schmidt *et al.* (2008), the atomistic origin of the piezoelectric effect has so far been investigated for only a very narrow class of compounds. Moreover, the fundamental relationship between the atomic arrangement, the electron-density distribution and piezoelectric properties can not be explained in full detail for any single structure (Hansen *et al.*, 2004). In this context, X-ray diffraction under an external electric perturbation turns out to be a promising experimental tool for obtaining an understanding of the piezoelectric effect at the microscopic level. The great advantage of this technique is that the atomic movements caused by the electric field and the corresponding macroscopic deformations (external strains) can be simultaneously and separately studied using one and the same sample. The small displacements of the atomic positions in the unit cell [internal strains, $\Delta R \sim 10^{-4}$ Å (Gorfman *et al.*, 2006)] may be evaluated from Bragg intensity changes. The external strains also manifest themselves as small angular shifts of diffraction curves [$\Delta\omega \sim 10^{-3\circ}$ (Gorfman *et al.*, 2007)].

In a recent study (Gorfman *et al.*, 2006) we investigated the internal strains in a piezoelectric ternary α-$GaPO_4$ crystal and analyzed the related distortions of chemical bonds induced by an applied electric field. The interpretation of the specific response of both the Ga—O and P—O bonds was based on the results of a topological analysis of the static electron density. It revealed that the P—O bonds were slightly more deformed by the external electric field than the Ga—O bonds. The aim of the present work is to extend this experiment to $Li_2SO_4{\cdot}H_2O$ by investigating the behavior of the Li—O/S—O bonds under an external electric perturbation. Li compounds are of interest for many applications, such as Li batteries (Nagel *et al.*, 2002) or ion conductors (Deiseroth *et al.*, 2008).

$Li_2SO_4{\cdot}H_2O$ is a polar crystal with interesting physical properties. It has the highest pyroelectric coefficient of all non-ferroelectric crystals [$p_2 = 87\ (2) \times 10^{-6}$ C m^{-2} K^{-1} (Becker *et al.*, 2003)]. The highest piezoelectric constant of $Li_2SO_4{\cdot}H_2O$ is the longitudinal component [d_{222} = 15.8 (5) pC N^{-1} (Ochrombel, 2007)], which is about seven times larger than that of α-quartz (d_{111} = 2.3 pC N^{-1}). Another reason why this crystal was chosen for the present studies is the availability of large single crystals of excellent quality grown from water solution (Wilke & Bohm, 1988).

In §2 we report on the multipole-model refinement of the electron density in $Li_2SO_4{\cdot}H_2O$. §3 deals with the measurement of the angular shifts and intensity variations of diffraction curves under the influence of an external electric field. The model used for calculating the atomic displacements within the unit cell of $Li_2SO_4{\cdot}H_2O$ is described in §4. The application of the model and the results of the refinement are presented in §5.

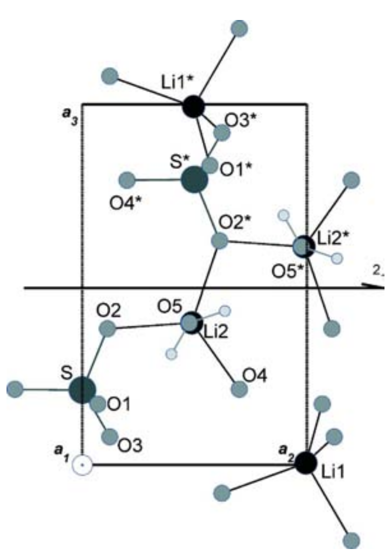

Figure 1
Arrangement of the LiO_4, $LiO_3(H_2O)$ and SO_4 tetrahedra in the $Li_2SO_4{\cdot}H_2O$ crystal structure viewed along the [100] crystallographic direction. The symmetry operation $[-x, y + 1/2, -z]$ relates atoms with their symmetry equivalents, which are marked by stars. In addition, the direction of the twofold screw axis parallel to [010], the monoclinic basis vectors and the corresponding unit cell are shown.

2. Electron density and properties of the chemical bonds in $Li_2SO_4{\cdot}H_2O$

The experimental electron-density (ED) distribution in $Li_2SO_4{\cdot}H_2O$ is required for the evaluation of the chemical-bond properties. The crystal structure and thermal motion in $Li_2SO_4{\cdot}H_2O$ have been reported by Ziegler (1934), Larson (1965) and Lundgren *et al.* (1984). Although the ED in $Li_2SO_4{\cdot}H_2O$ has already been studied (Karppinen *et al.*, 1986), no quantitative analysis of the particular properties of the Li—O and S—O chemical bonds has been made using modern tools such as Bader topological analysis (Bader, 1990).

$Li_2SO_4{\cdot}H_2O$ crystallizes in the space group $P2_1$ [unit-cell parameters a = 5.4553 (1), b = 4.8690 (1), c = 8.1761 (1) Å, β = 107.337 (2)° (Karppinen *et al.*, 1986)]. The asymmetric part of the unit cell consists of ten atoms: two Li atoms (Li1, Li2), one S atom (S), five O atoms (O1 to O5) and two H atoms (H1, H2). Each atom occupies a general (2a) position. The crystal structure is formed by LiO_4, $LiO_3(H_2O)$ and SO_4 groups, which are linked together by O atoms to form a three-dimensional tetrahedral framework, as shown in Fig. 1.

For the ED determination we prepared a spherical sample with a radius of 0.12 (1) mm. X-ray diffraction measurements were collected using an Enraf–Nonius CAD-4 diffractometer and Mo $K\alpha$ radiation. The sample was cooled to a temperature of 90 (5) K by an N_2 jet. The intensities of Bragg reflections were recorded with a point detector in an ω–2θ scan mode. The measurement time for each rocking curve was individually adjusted to ensure that the uncertainty in the intensity was less than 1.0%. However, for weak reflections the time was restricted to 10 min. In total over about three weeks 7853 reflections up to $\sin\theta/\lambda$ = 1.2 Å^{-1} fulfilling the condition $I(\mathbf{H}) > 3\sigma(I)$ were collected (see Table 1).[1] Using the software *Jana2000* (Petricek & Dusek, 2000), we corrected the data for the decay, Lorentz–polarization and absorption effects, merged the intensities of symmetry-equivalent reflections and finally submitted them to the refinement program *MOLLYN* (Guillot & Hansen, 2003).

The initial values of the atomic positions and ADPs were taken from the work of Karppinen *et al.* (1986) and were further refined without any constraints. The ADPs of the H atoms were fixed at their 80 K neutron-diffraction values (Lundgren *et al.*, 1984). The primary and secondary extinction were refined in the isotropic approximation according to Becker & Coppens (1974). In total 65 outlier reflections [having $|I_{OBS} - I_{MOD}|/\sigma(I_{OBS}) > 10$] and reflections heavily

[1] Supplementary data for this article are available from the IUCr electronic archives (Reference: SH5086). Services for accessing these data are described at the back of the journal.

Table 1
Data collection and multipole refinement of the ED in $Li_2SO_4{\cdot}H_2O$.

Experimental parameters	
Radiation type	Mo $K\alpha$
Detection type	Point detector
Temperature (K)	90 (5)
Radius of crystal sphere (mm)	0.12 (1)
μ (mm^{-1})	0.68 (1)
Recorded data	
$(\sin\theta/\lambda)_{max}$ (Å^{-1})	1.2
Observed/unique reflections	7853/3930
Redundancy	2
R_{int}†	0.028
Multipole refinement	
No. of ED parameters	48
Omitted reflections	65
$R_{IAM}(F)$‡	0.0150
$R(F)/R_w(F)$§	0.0143/0.0179
Goodness of fit¶	5.18

† Internal agreement factor (Petricek & Dusek, 2000). ‡ Independent atoms model (Guillot & Hansen, 2003). § Multipole model (Guillot & Hansen, 2003). ¶ Guillot & Hansen (2003).

affected by extinction (y_{ext} < 85% and $I_{OBS} = y_{ext}I_{KIN}$, where I_{KIN} is the diffraction intensity predicted within the kinematical theory) were omitted from the data set. Using scattering factors for isolated atoms, the refinement of these structural parameters resulted in the reliability factor R_{IAM} = 1.50%. As a next step we refined the multipole-model parameters. This model was introduced by Hansen & Coppens (1978) and is based on the pseudoatomic multipolar expansion of the ED of a single atom μ:

$$\rho_\mu(\mathbf{r}) = \rho_{core}(r) + P_{val}\kappa'^3\rho_{val}(\kappa' r) + \sum_{l=0}^{l_{max}}\kappa''^3 R_l(\kappa'' r)\sum_{m=0}^{l}P_{lm\pm}d_{lm\pm}(\mathbf{r}/r). \quad (1)$$

Here the spherical core and valence densities $\rho_{core}(r)$ and $\rho_{val}(\kappa' r)$ of a pseudoatom are calculated from the nonrelativistic ground-state Hartree–Fock wavefunctions for isolated atoms (Clementi & Roetti, 1974), and P_{val} and P_{lm} are the refined multipole population coefficients. The radial expansion–contraction is described by the parameters κ' and κ''.

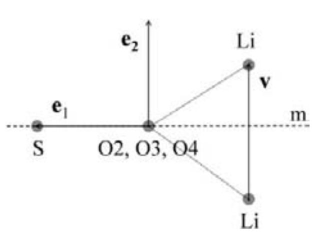

Figure 2
The next-neighbor coordination of the O2, O3 and O4 atoms in the $Li_2SO_4{\cdot}H_2O$ structure and the choice of their respective local Cartesian coordinate systems, $\{\mathbf{e}_i\}$. The axis $\mathbf{e}_1$ is directed from O to the corresponding S atom. The axis $\mathbf{e}_2$ lies in the $\mathbf{e}_1$–$\mathbf{v}$ plane ($\mathbf{v}$ is the vector between the Li atoms) and defines the normal to the local noncrystallographic mirror plane. The angle between $\mathbf{v}$ and $\mathbf{e}_2$ for the O2, O3 and O4 atoms is less than 5°.

$R_l(r)$ are the Slater-type radial functions [see *e.g.* Tsirelson & Ozerov (1996)] and $d_{lm\pm}(\mathbf{r}/r)$ are real spherical harmonics.

In order to reduce the number of ED parameters, we included noncrystallographic local symmetry elements for the positions of the Li1, Li2, S, O2, O3, O4 and O5 atoms. In particular, since the S and both Li atoms occupy positions in the center of slightly distorted oxygen tetrahedra, only the multipoles allowed by the tetrahedral symmetry $\overline{4}3m$ were considered for these three atoms. Furthermore, for Li1 and Li2 equal multipole populations and contraction coefficients κ' were used (refinement of κ'' did not result in convergence). Since the O atoms O2, O3 and O4 are almost equally coordinated by one S and two Li atoms (see Fig. 2) they may be constrained to be chemically equivalent. Therefore for these three atoms we refined one set of the multipole population coefficients and only those that are allowed under the local noncrystallographic mirror plane. The local Cartesian coordinate systems of the O2, O3 and O4 atoms were chosen such that the X axis ($\mathbf{e}_1$) points from the respective O atom towards the corresponding S atom. The Y axis ($\mathbf{e}_2$) is almost parallel to a line connecting the two next-neighbor Li atoms and normal to the local mirror plane introduced above (as shown in Fig. 2). Because the O atom O5 is linked to one Li and two H atoms, it was treated in a similar way to O2, O3 and O4 with a noncrystallographic mirror plane located between the H atoms. For all the O atoms only the P_{lm} up to l = 3 were included in the multipole-model refinement; the inclusion of hexadecapoles did not improve the fit. For the two symmetry-independent H atoms only one (and the same) single valence-shell dipole population (P_{10}) was taken into account. The corresponding dipole redistribution of the ED describes the formation of the chemical bonds between the H and O5 atom. With all these constraints the total number of ED parameters could be reduced to 48.

The results of the multipole refinement are presented in Figs. 3 and 4, showing the difference ED maps, *i.e.* the difference between the crystal ED (multipole density) and the density calculated by the superposition of isolated atoms (IAM density),

$$\Delta\rho(\mathbf{r}) = V^{-1}\sum_{\mathbf{H}}\big[|F_{OBS}(\mathbf{H})|\exp(i\varphi_{MULT}) - |F_{IAM}(\mathbf{H})|\exp(i\varphi_{IAM})\big]\exp(-2\pi i\mathbf{Hr}),$$

within the O1—S—O3 and O3—Li1—O4 planes. The pronounced features of the residual ED,

$$\Delta\rho(\mathbf{r}) = V^{-1}\sum_{\mathbf{H}}\big(|F_{OBS}(\mathbf{H})| - |F_{MULT}(\mathbf{H})|\big)\exp(i\varphi_{MULT}) \times \exp(-2\pi i\mathbf{Hr}),$$

(those greater than 0.1 e Å^{-3}) (Fig. 5) are localized near the sulfur nucleus, reflecting the typical difficulties in the description of the inner-core electrons of this atom (Coppens, 1997).

We used the program *WinXPRO* (Stash & Tsirelson, 2002) to perform the topological analysis of the experimental ED in $Li_2SO_4{\cdot}H_2O$. The ED at the (3, −1) bond critical points, ρ_{BCP}, of the SO_4, $Li1O_4$ and $Li2O_4$ groups and the atomic charges,

Table 2
Experimental values of the ED, Laplacian, eigenvalues of the Hessian matrix and the total energy density at the S—O, Li1—O and Li2—O bond critical points averaged over the bonds within the SO_4, $Li1O_4$ and $Li2O_4$ tetrahedra.

Tetrahedron	$\langle\rho_{BCP}\rangle$ (e Å^{-3})	$\langle\nabla^2\rho_{BCP}\rangle$ (e Å^{-5})	λ_1 (e Å^{-5})	λ_2 (e Å^{-5})	λ_3 (e Å^{-5})	h (a.u.)
SO_4	1.90	8.61	−12.98	−12.82	34.33	−0.316
$Li1O_4$	0.15	4.60	−0.95	−0.94	6.37	0.011
$Li2O_4$	0.17	5.15	−1.17	−1.12	7.39	0.012

Table 3
Theoretical values of the ED, Laplacian, eigenvalues of the Hessian matrix and the total energy density at the S—O, Li1—O and Li2—O bond critical points averaged over the bonds within the SO_4, $Li1O_4$ and $Li2O_4$ tetrahedra.

Tetrahedron	$\langle\rho_{BCP}\rangle$ (e Å^{-3})	$\langle\nabla^2\rho_{BCP}\rangle$ (e Å^{-5})	λ_1 (e Å^{-5})	λ_2 (e Å^{-5})	λ_3 (e Å^{-5})	h (a.u.)
SO_4	1.99	−2.81	−13.54	−13.51	24.24	−0.384
$Li1O_4$	0.17	4.38	−1.03	−1.01	6.42	0.009
$Li2O_4$	0.19	6.26	−0.94	−1.06	8.27	0.014

Table 4
Pseudoatomic charges in $Li_2SO_4{\cdot}H_2O$.

Values are calculated according to Bader (1990) on the basis of experimental and theoretical electron densities.

	S	Li1	Li2	O1	O2	O3	O4	O5	H1	H2
Q_{EXP} (e)	4.40	0.91	0.90	−1.34	−1.36	−1.42	−1.38	−1.59	0.45	0.48
Q_{WIEN2k} (e)	4.13	0.86	0.86	−1.43	−1.46	−1.46	−1.45	−1.35	0.67	0.67

Q, were determined according to the Bader formalism (Bader, 1990) (see Tables 2 and 4). In addition, we looked at the Laplacians of the ED, $\nabla^2\rho$, the Hessian matrix eigenvalues, λ_1, λ_2 and λ_3, and the total energy density, h, at the bond critical points.

The features of the experimental ED that were obtained were crosschecked by theoretical calculations with the DFT program package *WIEN2k* (Blaha *et al.*, 2001). As shown in Tables 2, 3 and 4, the agreement between the theoretical and experimental results is reasonable. However, in the case of the S—O bonds there is a big discrepancy in the eigenvalue λ_3 of the Hessian matrix and in the sign of the respective Laplacian. For the second-row atoms, like S, the dominating influence of λ_3 on the value of the Laplacian, $\nabla^2\rho = \lambda_1 + \lambda_2 + \lambda_3$, was also noted by Coppens (1997). The negative sign of the total energy density at the S—O critical points (Tsirelson & Stash, 2004; Gatti, 2005) indicates either covalent ($\nabla^2\rho < 0$, as follows from *WIEN2k* calculations) or intermediate bond interactions (between closed-shell and shared interactions, $\nabla^2\rho > 0$, as follows from the multipolar refinement). A closed-shell type of interaction ($h > 0$ and $\nabla^2\rho > 0$) was deduced for the Li—O bonds.

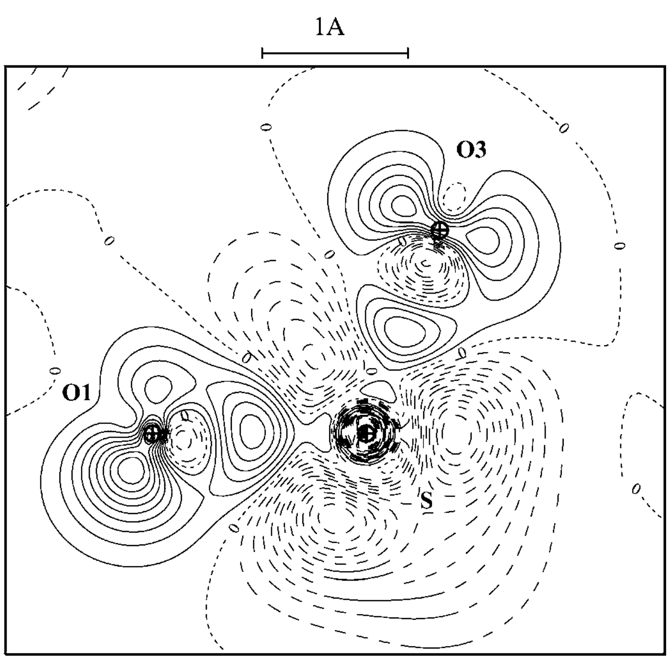

Figure 3
Difference ED within the O1—S—O3 plane. Contour intervals are at 0.05 e Å^{-3}, broken lines represent negative contours.

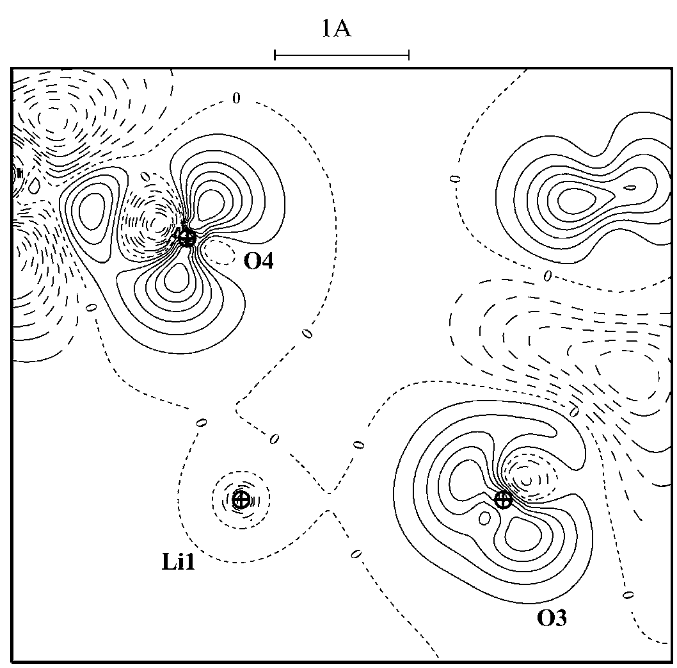

Figure 4
Difference ED within the O3—Li1—O4 plane. Contours are as in Fig. 3.

3. X-ray diffraction study of $Li_2SO_4{\cdot}H_2O$ under the influence of an applied external electric field

The experiment presented in this section was performed using a 0.590 (2) mm thick $Li_2SO_4{\cdot}H_2O$ (010) crystal plate (1.5 × 1.7 cm surface area) cut from a large right-handed single crystal. The crystal morphology allows the distinction between the left and right forms, and physically the handedness can be recognized from the sign of the longitudinal piezoelectric constant d_{222}, see *e.g.* Bohatý *et al.* (2005). Thus we ensured that the crystal investigated by X-ray diffraction under an external electric field had the same handedness as the crystal used for the ED studies (see §2). We created a homogeneous external electric field normal to the plate surface by supplying a high voltage to vacuum-evaporated thin gold contacts lying exactly in line with each other on opposite faces (0 ±1 0) of the crystal. The high voltage that was applied was periodically modulated with a frequency of 18 Hz through alternating positive (U_+), zero (U_0), negative ($U_- = -U_+$) and zero step states (Puget & Godefroy, 1975). The diffraction signals from the detector were continuously distributed over four counting channels, synchronized with the modulation of the high voltage. In this way the intensity of the diffracted X-ray beam can be measured quasi-simultaneously for each of the three different electric field states (see Fig. 6).

The measurements were performed at the D3 beamline of HASYLAB using a Huber four-circle diffractometer equipped with an NaI(Tl) scintillation counter. Selected diffraction curves were recorded at the wavelength λ = 0.6 Å by rocking the crystal about the exact Bragg positions (ω scans). To evaluate the angular shifts of peak positions

$$\Delta\omega_E = \omega_0(E) - \omega_0(E=0) \tag{2}$$

all diffraction profiles were fitted using a pseudo-Voigt function (Angel, 2003). The relative variations of Bragg intensities under an applied electric field of E = 5.1 kV mm^{-1} were extracted from single rocking curves. The uncertainties, $\sigma(\Delta I/I)$, were calculated on the basis of Poisson statistics:

$$\left(\frac{\Delta I}{I}\right)_E = \frac{I_E - I_{E=0}}{I_{E=0}}, \quad \sigma\left(\frac{\Delta I}{I}\right) \simeq \frac{1.22}{N_0^{1/2}}. \tag{3}$$

In general, a measurement of a single reflection was repeated until the total number of counts N_0 was high enough to provide $\sigma(\Delta I/I)$ of the order of 0.1%.

In the case of $Li_2SO_4{\cdot}H_2O$ the intensities of selected Bragg reflections may be particularly sensitive to the electric-field-generated internal strains. For example, the reflection $50\overline{6}$ exhibits an effect of $\Delta I/I \simeq 8\%$ (see Fig. 7), which is remarkably high for this kind of experiment (usually the measured relative intensity variation is of the order of 1%). Furthermore, the $\Delta I/I$ values of this reflection show a good linear dependence on the magnitude of the external electric field (Fig. 8). Note that in this range of the electric field strength a linear behavior of the intensity variations was observed in almost all previous experiments (Davaasambuu *et al.*, 2003; Gorfman *et al.*, 2006).

Finally, for all further data treatment we normalized the observed angular shifts and relative intensity variations to the values referred to the electric field $\mathbf{E}_+ = 5.1\mathbf{e}_2$ kV mm^{-1} applied in the positive [010] direction:

$$\Delta\omega_{\rm a} = \langle \Delta\omega_{E_+}, -\Delta\omega_{E_-}\rangle,$$
$$(\Delta I/I)_{\rm a} = \langle (\Delta I/I)_{E_+}, -(\Delta I/I)_{E_-}\rangle. \tag{4}$$

As the experiment was time consuming, we employed a special strategy for the data collection. For the initial measurement period we compiled a list of Bragg reflections whose intensities were predicted to be highly sensitive to the *a priori* pseudoatomic displacements. The latter were estimated by applying a model of independent atomic vibrations as described by Gorfman *et al.* (2005). In this way we collected 43 reflections showing a measurable effect in $\Delta I/I$ and exploited them for preliminary refinement (the details of the model are presented in §4). The average relative change of the Bragg intensities observed during the first measurement, $\langle|(\Delta I/I)_{\rm a}|\rangle$,

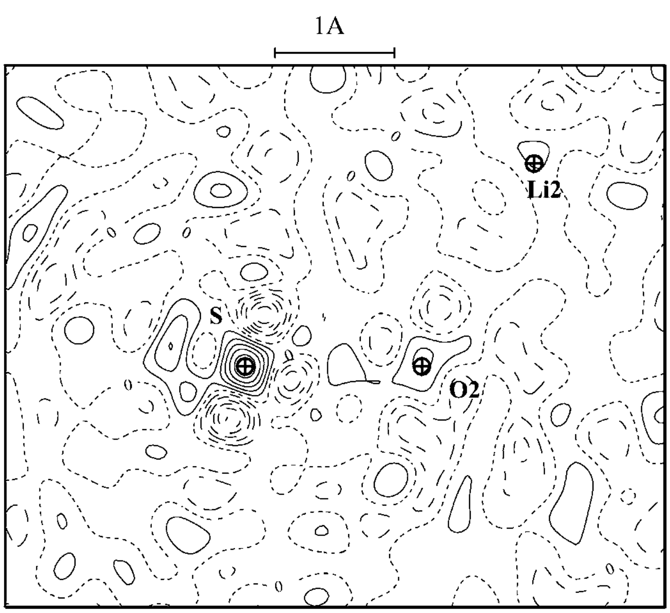

Figure 5
Residual ED map within the S—O2—Li2 plane (contours are as in Fig. 3).

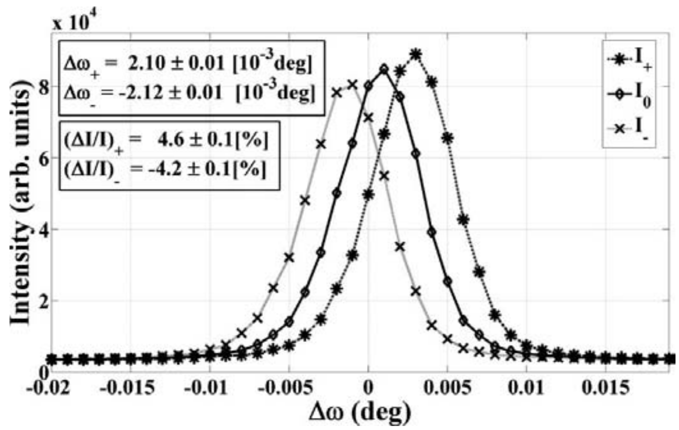

Figure 6
The ω rocking curves (I_+, I_0 and I_-) of a $0,\overline{1},12$ reflection corresponding to the U_+, U_0 and U_- states of the high voltage ($|U_\pm|$ = 3 kV).

was about 1.0%. Using the roughly refined pseudoatomic shifts we created a new list of reflections and collected 71 more $(\Delta I/I)_{\rm a}$ values (as summarized in Fig. 9; $\langle|(\Delta I/I)_{\rm a}|\rangle \simeq 2.1\%$). Finally both sets were merged to a single data pool which was submitted to the final model refinement.

4. Model used for the description of the electric-field-induced pseudoatomic displacements in $Li_2SO_4{\cdot}H_2O$

The intensity of the X-ray diffraction by a crystal in the presence of an applied external electric field has been analyzed by Tsirelson *et al.* (2003) and Gorfman *et al.* (2005). They showed that the change of the kinematical diffraction intensities is mainly due to the electric-field-induced displacements of pseudoatoms within the crystal unit cell. The contribution of the electron subsystem polarization is estimated as 100 times smaller and thus can be neglected. The structure factor of a crystal under an applied external electric field takes the form

$$F_E(\mathbf{H}) = \sum_\mu \left[f_\mu(\mathbf{H}) + f'_\mu(\lambda) + if''_\mu(\lambda)\right] \times T_\mu(\mathbf{H}) \exp\{2\pi i \mathbf{H}\mathbf{R}_\mu\} \exp\{2\pi i \mathbf{H}\Delta\mathbf{R}_\mu(\mathbf{E})\}, \quad (5)$$

where $\mathbf{H}$ is a reciprocal-lattice vector, f_μ, f'_μ and f''_μ are the atomic and anomalous scattering factors, respectively, $\mathbf{R}_\mu$ represent the original atomic positions and T_μ represent the temperature factors. The pseudoatomic displacement vectors, $\Delta\mathbf{R}_\mu$, are the parameters of the model intensity variations $((\Delta I/I)_{\rm a})_{\rm MOD}$,

$$((\Delta I/I)_{\rm a})_{\rm MOD} = \frac{|F_E|^2 - |F_{E=0}|^2}{|F_{E=0}|^2}, \quad (6)$$

and are refined by minimizing the error sum:

$$\chi^2 = \sum_{\mathbf{H}} \left[\frac{((\Delta I/I)_{\rm a})_{\rm OBS} - ((\Delta I/I)_{\rm a})_{\rm MOD}}{\sigma((\Delta I/I)_{\rm a})}\right]. \quad (7)$$

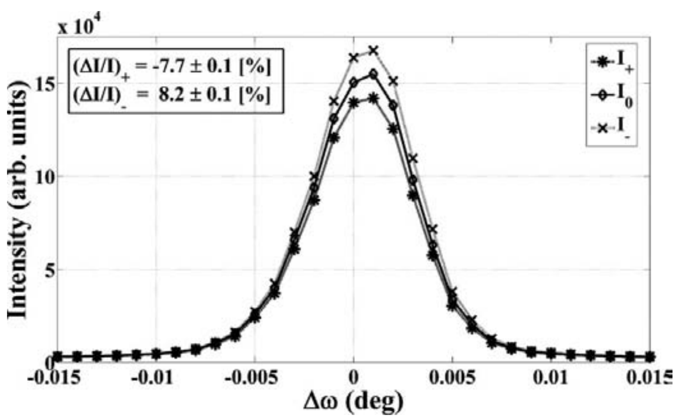

Figure 7
Three rocking curves of the $50\overline{6}$ reflection measured at positive, zero and negative voltage applied to the crystal. The structure factor of this reflection is unusually highly sensitive to the small shifts of the atomic positions induced by an external electric field parallel to the [010] direction.

In a linear approximation the components ΔR^i_μ (referred to the crystallographic coordinate system and marked by a superscript i) of the $\Delta\mathbf{R}_\mu$ vectors are described as

$$\Delta R^i_\mu = \left[a^i_j(\mu)\right]E^j; \quad (8)$$

the Einstein summation rule holds. The displacement tensor $\hat{\mathbf{a}}$, with components $a^i_j(\mu)$, and its dependence on the microscopic parameters of the crystal, such as phonon spectra and ED distribution, were discussed by Gorfman *et al.* (2006). Note that $\hat{\mathbf{a}}(\mu^*)$ of an atom μ^* which is related to an atom μ by the symmetry operation $\{\mathbf{S}, \mathbf{d}\}$ ($\mathbf{S}$ is a rotation matrix and $\mathbf{d}$ is a translation vector) is given by

$$\left[a^i_j(\mu^*)\right] = \mathbf{S}\left[a^i_j(\mu)\right]\mathbf{S}^{-1}. \quad (9)$$

In the case of $Li_2SO_4{\cdot}H_2O$ the only symmetry operation that is not just a pure lattice translation is a 2_1 screw axis parallel to $\mathbf{a}_2$, therefore the components of $\hat{\mathbf{a}}(\mu^*)$ [equation (9)] in the crystallographic coordinate system are given by

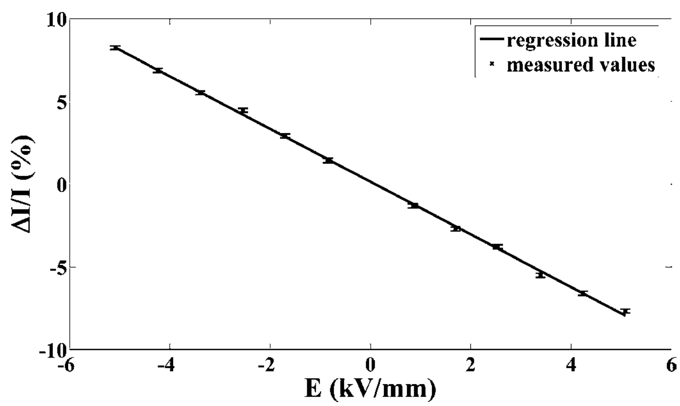

Figure 8
Values of the relative intensity change, $\Delta I/I$, of the $50\overline{6}$ reflection measured as a function of the magnitude of the applied electric field. This measurement confirms the assumption that the microscopic crystal response is linear within the high-voltage range considered.

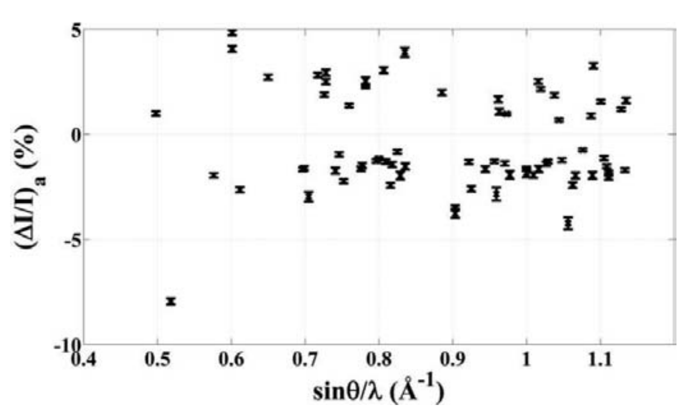

Figure 9
All $(\Delta I/I)_{\rm a}$ values recorded during the second measurement plotted against $\sin\theta/\lambda$.

$$\left[a_j^i(\mu^*)\right] = \begin{pmatrix} a_1^1 & -a_2^1 & a_3^1 \\ -a_1^2 & a_2^2 & -a_3^2 \\ a_1^3 & -a_2^3 & a_3^3 \end{pmatrix}$$

$$\text{with} \quad \left[a_j^i(\mu)\right] = \begin{pmatrix} a_1^1 & a_2^1 & a_3^1 \\ a_1^2 & a_2^2 & a_3^2 \\ a_1^3 & a_2^3 & a_3^3 \end{pmatrix}. \qquad (10)$$

In our experiment we applied the external electric field in the [010] crystallographic direction only. According to equation (8) the parameters that have to be refined are the second columns of equation (10), $a_2^i(\mu)$, belonging to symmetry-independent atoms. Therefore an unconstrained model should contain 30 independent parameters (three for each atom in the asymmetric unit of $Li_2SO_4 \cdot H_2O$).

We did not refine the displacements of the H atoms ($\Delta\mathbf{R}_{H1} = \Delta\mathbf{R}_{H2} = 0$) as their scattering power is too small to yield any significant results. Considering the relatively small scattering power of the Li atoms, we constrained their shifts to be equal to each other and parallel to the external electric field. The reason behind this assumption originates from the relatively weak Li—O bonds:

$$\Delta\mathbf{R}_{Li1} = \Delta\mathbf{R}_{Li2} = a_{Li}\mathbf{E}, \text{ with } \Delta\mathbf{R}_{Li}, \mathbf{E} \parallel \mathbf{a}_2. \qquad (11)$$

The displacements of O2, O3 and O4 were restrained according to the local noncrystallographic mirror planes introduced in §2. In addition, the chemical-equivalence condition was imposed on these atoms, so that the components of the displacement tensors $\hat{\mathbf{a}}$(O2), $\hat{\mathbf{a}}$(O3) and $\hat{\mathbf{a}}$(O4) in the respective atomic local Cartesian coordinate system (Fig. 2) are equal to each other and take the form

$$[a_{ij}(\mathrm{O})] = \begin{pmatrix} \alpha_{11} & 0 & \alpha_{13} \\ 0 & \alpha_{22} & 0 \\ \alpha_{31} & 0 & \alpha_{33} \end{pmatrix}. \qquad (12)$$

The special form of equation (12) is due to the noncrystallographic mirror plane, related to the atomic positions of O2, O3 and O4. To express the components of $\hat{\mathbf{a}}$(O) in the crystallographic coordinate system we introduced the matrix of transformation $\mathbf{A}(\mathrm{O}_\mu)$ from the local Cartesian coordinate system of an atom O_μ to the global crystallographic coordinate system, $\{\mathbf{a}_j\}$:

$$\left[a_j^i(\mathrm{O}_\mu)\right] = \mathbf{A}(\mathrm{O}_\mu)[a_{ij}(\mathrm{O})]\mathbf{A}^{-1}(\mathrm{O}_\mu). \qquad (13)$$

The five elements α_{11}, α_{13}, α_{22}, α_{31} and α_{33} from equation (12) are the only parameters in the refinement. Thus the number of variables describing the displacements of O2, O3 and O4 could be reduced from 9 to 5.

Furthermore, we took into account the fact that the translation of all atoms by the same vector does not affect the absolute value of the structure factor, $|F_E|$. To exclude this ambiguity of the results we put an additional constraint on the quantities $\Delta\mathbf{R}_\mu$ (Gorfman *et al.*, 2006):

$$\sum_\mu \Delta\mathbf{R}_\mu = 0. \qquad (14)$$

Here the sum runs over all atoms within the unit cell. As follows from equation (10), the first and the third components of the vector sum [equation (14)] (relative to the crystallographic coordinate system) automatically cancel for the displacements of a pair of symmetry-equivalent atoms (for the electric field $\mathbf{E} \parallel \mathbf{a}_2$ $\Delta R^1 = -\Delta R^{1*}$, $\Delta R^2 = \Delta R^{2*}$, $\Delta R^3 = -\Delta R^{3*}$). Therefore the condition given in equation (14) is relevant for the second components ΔR_μ^2 only and effectively reduces the number of free parameters by one.

Finally, we considered the macroscopic dielectric polarization of the crystal, $\Delta\mathbf{P}$, induced by the applied electric field, $\mathbf{E}$. On the one hand $\Delta\mathbf{P}$ may be expressed *via* pseudoatomic charges and shifts of the atoms in the unit cell. On the other hand $\Delta\mathbf{P}$ is described by the low-frequency dielectric tensor, $\hat{\boldsymbol{\varepsilon}}$, whose components in $Li_2SO_4 \cdot H_2O$ were published some time ago by Mason (1952). Assuming that the atomic displacements provide the main contribution to $\Delta\mathbf{P}$, both approaches are equal to each other, so

$$(\hat{\boldsymbol{\varepsilon}} - 1)\mathbf{E} = \sum_\mu Q_\mu \Delta\mathbf{R}_\mu/(\varepsilon_0 V). \qquad (15)$$

In the above equation ε_0 is the vacuum susceptibility, Q_μ is the pseudoatomic charge of the μth atom in the unit cell (as given in the first row of Table 4) and V is the unit-cell volume. For calculating the right-hand side of equation (15) both H atoms were assumed to be rigidly shifted with O5. Under this and the other constraints that were introduced, the electric-field-induced atomic displacements in the $Li_2SO_4 \cdot H_2O$ structure are described by 13 parameters.

5. Refinement of the piezoelectric constants d_{2jk} and atomic displacements

Firstly, the angular shifts of the X-ray diffraction peaks, $\Delta\omega_a$ [equation (4)], were used to determine the piezoelectric constants d_{2jk} of $Li_2SO_4 \cdot H_2O$. An approach relating the mechanical strains with the $\Delta\omega_a$ values of an arbitrary set of reflections was introduced by Graafsma (1992) and further developed by Gorfman *et al.* (2007). According to this approach, the shift of an ω rocking curve induced by an external electric field $\mathbf{E}$ applied to a crystal possessing the piezoelectric constants d_{ijk} is given by

$$\Delta\omega_a = -\tan(\theta) d_{ijk} E_i H_j H_k / H^2 - d_{ijk} E_i Y_j H_k / H + R_{ijk} E_i Y_j H_k / H. \qquad (16)$$

In this equation θ is the Bragg angle and H_i are the components of the reciprocal-lattice vector $\mathbf{H}$ related to the crystal Cartesian system. The unit vector $\mathbf{Y}$ is defined as $\mathbf{Y} = [\mathbf{H}, \boldsymbol{\omega}/H]$, where $\boldsymbol{\omega}$ denotes the unit direction of the rotation axis of the diffractometer. With the second-rank tensor $R_{ijk}E_i$ the rotation of the whole crystal plate caused by $\mathbf{E}$ is described.

As illustrated in Fig. 10, no more than 20 different reflections have to be submitted to the refinement procedure in order to get reliable values for the four piezoelectric constants d_{2jk} (d_{211}, d_{222}, d_{233} and d_{213}). Adding further data did not change the refined values of the constants much. As the

Table 5
Piezoelectric constants d_{2jk}.

The piezoelectric constants d_{2jk} (10^{-12} mV^{-1}) of $Li_2SO_4{\cdot}H_2O$ determined in this work and macroscopically measured by means of a dynamical pressure cell (Ochrombel *et al.*, 2006) are compared.

	d_{211}	d_{222}	d_{233}	d_{213}
First data set	−3.26 (1)	15.17 (1)	1.16 (1)	−2.59 (1)
Second data set	−3.57 (1)	15.48 (1)	1.68 (1)	−2.29 (1)
Average of first and second data sets	−3.4 (3)	15.3 (2)	1.4 (3)	−2.4 (2)
Ochrombel (2007)	−3.3 (2)	15.8 (5)	1.7 (1)	−2.2 (1)

Table 6
Main parameters of the refinement of the electric-field-induced relative shifts of pseudoatoms in $Li_2SO_4{\cdot}H_2O$.

No. $(\Delta I/I)_a$ denotes the number of symmetry-independent reflections considered, R and R_w are the unweighted and weighted agreement indices.

No. $(\Delta I/I)_a$	No. of variables	R	R_w	$\langle\lvert\sigma/(\Delta I/I)_a\rvert\rangle$
104	13	0.25	0.25	0.13

rotation contribution [the third term in equation (16)] depends to a degree on how a crystal is fixed on the goniometer head, we refined the piezoelectric constants d_{2jk} for the two measurements separately. The results are summarized in Table 5; in the first two rows the d_{211}, d_{222}, d_{233} and d_{213} values refined from the first and second set of measurements are presented and in the third row the averaged values are displayed. In the last row of Table 5 the experimental values that were macroscopically measured using a dynamical pressure cell are given (Ochrombel, 2007). The two data sets are in quantitative agreement.

The final refinement of the electric-field-induced pseudoatomic displacements in $Li_2SO_4{\cdot}H_2O$ is summarized in Table 6. The data-to-variables ratio reaches the value of 8, which is quite high for this kind of experiment. The quality of the fitting procedure including the model introduced in §4 was characterized by the unweighted (R) and weighted (R_w) agreement factors. The refined displacements of single atoms, as listed in Table 7, were used to evaluate the average variations of the Li1—O, Li2—O and S—O bond lengths. The first row of Table 8 displays the magnitude of the bond deformation due to the variation of the fractional atomic coordinates only (internal strains). The second row demonstrates the same bond-length changes corrected by considering the converse piezoelectric effect, *i.e.* the distortion of the unit-cell dimensions (external strains in combination with internal strains). It shows that the major part of the deformation of the bond lengths is the internal strains. In conclusion, the ionic Li—O chemical bonds are significantly more strongly affected by an external electric field than the covalent S—O bonds.

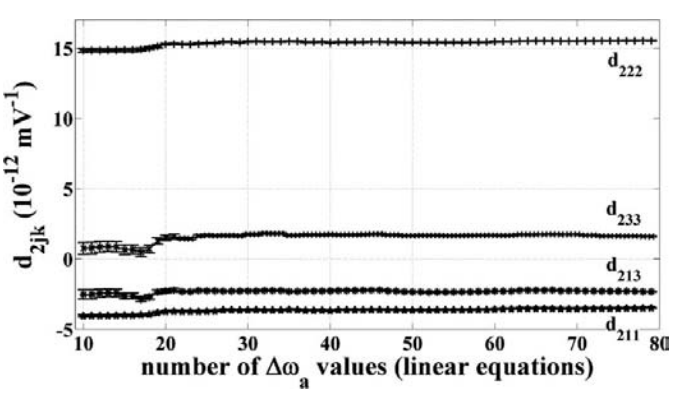

Figure 10
Four symmetry-allowed piezoelectric constants d_{2jk} (d_{211}, d_{222}, d_{233} and d_{213}) for the electric field applied parallel to the twofold axis of $Li_2SO_4{\cdot}H_2O$, refined as a function of the number of different reflections used at the same time in equation (16).

Table 7
Summary of the refined pseudoatomic displacements in $Li_2SO_4{\cdot}H_2O$ induced by an applied electric field of strength E = 5.1 kV mm^{-1}.

The components of the respective displacement vector, $\Delta\mathbf{R}$, are referred to the crystallographic system.

Atom(s)	ΔR^1 (10^{-5})	ΔR^2 (10^{-5})	ΔR^3 (10^{-5})
S	2.94 (2)	−2.49 (14)	0.35 (2)
Li1, Li2	0	17.67 (12)	0
O1	0.74 (7)	−5.93 (78)	−3.04 (9)
O2	−3.24 (2)	−1.99 (6)	0.98 (3)
O3	2.19 (14)	−9.28 (18)	0.62 (1)
O4	3.60 (9)	−1.03 (10)	2.53 (1)
O5	−4.20 (22)	−14.61 (33)	−6.12 (25)

Table 8
Measured electric-field-induced average variation of the cation–anion distances (Å × 10^5) in the three different structural units, LiO_4, $LiO_3(H_2O)$ and SO_4, of $Li_2SO_4{\cdot}H_2O$.

In the last row the influence of the converse piezoelectric effect (external strain) was taken into account. The values refer to the magnitude of the electric field E = 5.1 kV mm^{-1} (parallel to [010]).

	$\langle\lvert\Delta(\mathrm{Li1—O})\rvert\rangle$	$\langle\lvert\Delta(\mathrm{Li2—O})\rvert\rangle$	$\langle\lvert\Delta(\mathrm{S—O})\rvert\rangle$
Internal strain	58.5 (2)	52.4 (2)	8.3 (1)
Internal and external strain	60.9 (2)	55.0 (2)	6.3 (1)

6. Discussion

The distinctive bond-selective behavior of $Li_2SO_4{\cdot}H_2O$ under an external electric perturbation reflects the bond properties, characterized by means of the topological ED analysis (see Tables 2 and 4 in §2 for details). In particular, the value of the Bader charge of the S pseudoatom is by a factor of about 5 larger than that for the Li atoms. For this reason the effective force acting in an electric field on sulfur (*i.e.* the force on its atomic nucleus plus its pseudoatomic fragment of the ED) is stronger by the same factor. On the other hand, the average ED in the Li—O bond critical points is more than 10 times smaller than the corresponding value for the S—O bonds. This enormous difference is in qualitative agreement with the observed higher sensitivity of the LiO_4 and $LiO_3(H_2O)$ tetrahedra to the applied external electric field. At the same time, in spite of the higher charge of the pseudoatom S, the deformation of the SO_4 group is quite small, so that SO_4 remains almost rigid. This feature of the internal strain may originate from the nature of the S—O and Li—O bonds. As follows from the signs of the total energy density and Laplacians at the bond critical points (analyzed in §2), the interaction between the Li and O atoms is of a closed-shell (ionic) type. In contrast, the S—O bonds are either of covalent (see the *WIEN2k* calculations in Table 3) or intermediate (between closed-shell and shared) interactions (see the multipolar refinement in Table 2). Although we can not establish the type of interaction unambiguously, the charge density for both cases is mostly (for the covalent case) or partly (for the intermediate case) relocated to the bond region. Thus, the effective external electric force on the isolated pseudoatomic fragment becomes less dominant compared to the pure closed-shell interaction, which results in the small distortion of the S—O bond lengths: $\langle|\Delta(\mathrm{S-O})|\rangle/E = 1.2 \times 10^{-5}$ Å $(\mathrm{kV\,mm^{-1}})^{-1}$, whereas the variation of the Li—O bond lengths is quite high: $\langle|\Delta(\mathrm{Li-O})|\rangle/E = 11.3 \times 10^{-5}$ Å $(\mathrm{kV\,mm^{-1}})^{-1}$. Note that in our recent work on α-$GaPO_4$ (Gorfman *et al.*, 2006) we found similar magnitudes of the average Ga—O and P—O bond deformation under an external electric field: $\langle|\Delta(\mathrm{Ga-O})|\rangle/E = 1.8 \times 10^{-5}$ and $\langle|\Delta(\mathrm{P-O})|\rangle/E = 4.1 \times 10^{-5}$ Å $(\mathrm{kV\,mm^{-1}})^{-1}$.

We acknowledge the financial support of the Deutsche Forschungsgemeinschaft (SPP 1178/Experimental charge density determination as the key for understanding chemical interactions) and thank Dr Wolfgang Morgenroth for assistance with the experiments at the D3 beamline (HASYLAB, Hamburg).

References

Angel, R. J. (2003). *J. Appl. Cryst.* **36**, 295–300.
Bader, R. F. W. (1990). *Atoms in Molecules: A Quantum Theory*. Oxford University Press.
Becker, P., Ahrweiler, S., Held, P., Schneeberger, H. & Bohatý, L. (2003). *Cryst. Res. Technol.* **38**, 881–889.
Becker, P. J. & Coppens, P. (1974). *Acta Cryst.* A**30**, 129–147.
Blaha, P., Schwarz, K., Madsen, G. K. H., Kvasnicka, D. & Luitz, J. (2001). *WIEN2k. An Augmented Plane Waves + Local Orbital Program for Calculating Crystal Properties.* Technische Universität, Wien, Austria.
Bohatý, L., Becker, P., Eichler, H. J., Hanuza, J., Maczka, M., Takaichi, K., Ueda, K. & Kaminskii, A. A. (2005). *Laser Phys.* **15**, 1509–1522.
Clementi, E. & Roetti, C. (1974). *At. Data Nucl. Data Tables*, **14**, 177–478.
Coppens, P. (1997). *X-ray Charge Densities and Chemical Bonding.* New York: Oxford University Press.
Coppens, P. & Novozhilova, I. V. (2002). *Faraday Discuss.* **122**, 1–11.
Davaasambuu, J., Pucher, A., Kochin, V. & Pietsch, U. (2003). *Europhys. Lett.* **62**, 834–840.
Deiseroth, H. J., Kong, S. T., Eckert, H., Vannahme, J., Reiner, C., Zaiss, T. & Schlosser, M. (2008). *Angew. Chem. Int. Ed.* **47**, 755–758.
Fujimoto, I. (1978). *Phys. Rev. Lett.* **40**, 941–944.
Gatti, C. (2005). *Z. Kristallogr.* **220**, 399–457.
Gorfman, S., Schmidt, O., Pietsch, U., Becker, P. & Bohatý, L. (2007). *Z. Kristallogr.* **222**, 396–401.
Gorfman, S. V., Tsirelson, V. G. & Pietsch, U. (2005). *Acta Cryst.* A**61**, 387–396.
Gorfman, S., Tsirelson, V., Pucher, A., Morgenroth, W. & Pietsch, U. (2006). *Acta Cryst.* A**62**, 1–10.
Graafsma, H. (1992). *J. Appl. Cryst.* **25**, 372–376.
Graafsma, H., Coppens, P., Majewski, J. & Cahen, D. (1993). *J. Solid State Chem.* **105**, 520–527.
Guillot, R., Allé, P., Fertey, P., Hansen, N. K. & Elkaïm, E. (2002). *J. Appl. Cryst.* **35**, 360–363.
Guillot, R., Fertey, P., Hansen, N. K., Allé, P., Elkaim, E. & Lecomte, C. (2004). *Eur. Phys. J. B*, **42**, 373–380.
Guillot, R. & Hansen, N. K. (2003). *DIFMOL*. Internal computer programs of LCM3B, Université Henri Poincaré – Nancy I, France.
Hansen, N. K. & Coppens, P. (1978). *Acta Cryst.* A**34**, 909–921.
Hansen, N. K., Fertey, P. & Guillot, R. (2004). *Acta Cryst.* A**60**, 465–471.
Istomin, K., Kotaidis, V., Plech, V. & Kong, A. (2007). *Appl. Phys. Lett.* **90**, 022905.
Karppinen, M., Liminga, R., Lundgren, J.-O., Kvick, A. & Abrahams, S. C. (1986). *J. Phys. Chem.* **85**, 5521–5527.
Larson, A. C. (1965). *Acta Cryst.* **18**, 717–724.
Lundgren, J.-O., Kvick, A., Karppinen, M., Liminga, R. & Abrahams, S. C. (1984). *J. Phys. Chem.* **80**, 423–430.
Mason, W. P. (1952). *Piezoelectric Crystals and Their Application to Ultrasonics.* New York, Moscow: Van Nostrand.
Nagel, R., Gross, Th. W., Günther, H. & Lutz, H. D. (2002). *J. Solid State Chem.* **165**, 303–311.
Nye, J. F. (1957). *Physical Properties of Crystals.* Oxford: Clarendon Press.
Ochrombel, R. (2007). *Temperaturabhängige optische, elektrooptische und piezoelektrische Untersuchungen ausgewählter azentrischer Kristalle*. University of Cologne, Cologne, Germany.
Ochrombel, R., Lindner, M. & Bohatý, L. (2006). *Acta Cryst.* A**62**, s212.
Oganov, A. R., Glass, C. W. & Ona, S. (2006). *Earth Planet. Sci. Lett.* **241**, 95–103.
Paturle, A., Graafsma, H., Sheu, H.-S., Coppens, P. & Becker, P. (1991). *Phys. Rev. B*, **43**, 14683–14691.
Petricek, V. & Dusek, M. (2000). *JANA2000. The Crystallographic Computing System*. Institute of Physics, Praha, Czech Republic.
Puget, R. & Godefroy, L. (1975). *J. Appl. Cryst.* **8**, 297–303.
Reeuwijk, S. J. van, Puig-Molina, A. & Graafsma, H. (2001). *Phys. Rev. B*, **64**, 134105.
Schmidt, O., Gorfman, S. & Pietsch, U. (2008). *Cryst. Res. Technol.* **43**, 1126–1132.
Stahn, J., Pietsch, U., Blaha, P. & Schwarz, K. (2001). *Phys. Rev. B*, **63**, 165205.
Stash, A. & Tsirelson, V. (2002). *J. Appl. Cryst.* **35**, 371–373.
Tsirelson, V. & Stash, A. (2004). *Acta Cryst.* A**60**, 418–426.
Tsirelson, V. G., Gorfman, S. V. & Pietsch, U. (2003). *Acta Cryst.* A**59**, 221–227.
Tsirelson, V. G. & Ozerov, R. P. (1996). *Electron Density and Bonding in Crystals.* Bristol, Philadelphia: Institute of Physics Publishing.
Wilke, K.-Th. & Bohm, J. (1988). *Kristallzüchtung*. Berlin: VEB Deutscher Verlag der Wissenschaft.
Ziegler, G. E. (1934). *Z. Kristallogr.* **89**, 456–461.